# A comparative study of rheological evolution and crystallization kinetics of poly(ethylene terephthalate)

**Ph. Dumazet*, A. Douillard† and B. Chabert**
*Laboratoire d'Etudes des Matériaux Plastiques et des Biomatériaux, URA CNRS No. 507, Université 'Claude Bernard' Lyon I, 43 Boulevard du 11 Novembre 1918, 69622 Villeurbanne Cedex, France*

**and J. Guillet**
*Laboratoire de Rhéologie des Matières Plastiques, Université des Sciences, 23 Rue du Dr Paul Michelon, 42023 Saint Etienne Cedex 02, France*
*(Received 13 July 1992; revised 15 October 1993)*

The rheological behaviour of poly(ethylene terephthalate) (PET) is studied anisothermally at constant cooling rates (1 to 5°C min$^{-1}$) during crystallization from the melt. Drying conditions are first set up to keep the properties of the polymer constant (6 h at 150°C under vacuum). The modulus $\eta^*$ of the complex dynamic viscosity and the elastic component $G'$ of the complex elastic modulus are studied as functions of temperature in the linear domain and show a sigmoidal shape during the crystallization process. The starting temperature of each phenomenon is dependent on the cooling rate, and the values for $G'$ are always higher than the corresponding values for $\eta^*$. This fact can be explained by the higher sensitivity of $G'$ to the increasing number of entanglements in the early nucleation process. As the starting temperatures for $\eta^*$ are close to the values observed by differential scanning calorimetry (d.s.c.), an exhaustive study of this parameter is performed under various shearing conditions and interpreted by means of an experimental design. A second-order relation is then established and gives extrapolated starting temperature values for $\eta^*$ at low (or zero) shearing rates and frequencies in accordance with the d.s.c. values. Linear relationships between the starting temperatures of $\eta^*$, $G'$ and d.s.c. measurements, respectively, and the square root of the cooling rate are finally observed. As they show quite similar limiting temperature at zero cooling rates, it is assumed that a change of the crystallization or the nucleation process occurs at this point.

**(Keywords: poly(ethylene terephthalate); rheological kinetics; crystallization)**

## INTRODUCTION

During crystallization from the melt of a thermoplastic polymer, its rheological parameters, particularly the viscosity, present large variations, which can be useful for modelling the processing operations. The first step is the description of the crystallization kinetics, which has already been reported in a previous paper[1] for the polymer used here. The second stage is its correlation to the rheological evolution in the setting conditions. These parameters also influence the final morphology of the material and consequently the mechanical properties[2,3]. For crystallizable polymers, this topic has not yet been studied as exhaustively as for the viscosity increase of thermosets[4]. Concerning the isothermal crystallization of polyethylene, Lagasse and Maxwell[5] show that the early increase of viscosity corresponds to the first appearance of crystals in the molten phase. The shearing effect accelerates the kinetics only for high shearing rate values and gives afterwards fibrillar crystals. The induction period of the phenomenon is only shearing-rate-dependent and becomes shorter as the polymer network is extended between the temporary reticulation knots produced by the chain entanglements[6]. Heterogeneous particles can also induce a local orientation of the polymer chains, making the crystallization process easier[7,8].

Kushner and Chang[9] propose a method using an eccentric plane–plane rheometer for studying dynamic rheological kinetics. When it is applied to polyethylene, polyamide-11 and poly(butene terephthalate), the increase of the modulus of the dynamic complex viscosity for the elastic and viscous component is obvious during crystallization. Furthermore, we must notice that $\tan\delta$ decreases, which means that the sample becomes more and more elastic during crystallization. Moreover, a morphological study[10] leads to the conclusion that a higher nucleation rate occurs with shear and then reduces the induction time: for frequencies lower than 0.1 rad s$^{-1}$ a spherulitic structure is observed, which progressively disappears for higher values.

This paper is a contribution to the problem, generally called rheological kinetics, for poly(ethylene terephthalate) (PET); it is the continuation, in a comparative way, of

* Also at second address above
† To whom correspondence should be addressed

0032-3861/94/13/2828–06

the previous work concerning the crystallization kinetics of PET. In order to be in accordance with the normal polymer processing, an accurate model derived from the Avrami–Evans[11,12] relation was established for anisothermal conditions:

$$1-U=\exp\left[-K(T)\left(\frac{T_\alpha-T}{\alpha}\right)^n\right] \quad (1)$$

where $U$ is the volumic transformation rate; $\alpha>0$ is the cooling rate; $n$ and $K(T)$ are the Avrami coefficients; and $T_\alpha$ is the effective starting temperature of the kinetics. This last parameter depends on the rate $\alpha$ for quiescent conditions and can be qualitatively interpreted in terms of nucleation delay. Thus in the case of stresses during crystallization, the influence of the shearing strain and of the frequencies $\omega$ on $T_\alpha$ must be taken into account as well as their possible correlative interactions.

## EXPERIMENTAL

We used two PET samples, referred to as A and B, supplied by Rhône-Poulenc and previously studied for their crystallization kinetics. From their characteristics, described later on, their respective molecular weights are $M_{wA}=39\,000$ and $M_{wB}=43\,000$, and the polymolecularity ratios are $I_{pA}=2$ and $I_{pB}=2.5$. Complementary viscosity measurements were made with a SEPEM automatic viscosimeter, according to the Mark–Houwink–Sakurada relation[13]:

$$[\eta]=4.68\times10^{-4}M_w^{0.68} \quad (2)$$

for 50/50 (vol) phenol/tetrachlorethane solutions.

A Rheometrics Dynamic Analyzer RDA 700 is used to determine the following rheological parameters: $|\eta^*|=(\eta'^2+\eta''^2)^{1/2}$, the modulus of the complex dynamic viscosity $\eta'-i\eta''$, simply denoted $\eta^*$; $G'$ and $G''$, the components of the complex elastic modulus $G^*=G'+iG''$; and $\tan\delta=G''/G'$, the tangent of the loss angle.

As the highest possible cooling rate for the system cannot exceed 15°C min$^{-1}$, only anisothermal kinetics were carried out because quenching is not efficient enough to allow us to make an isothermal study. In order to obtain the best linear cooling rates in the range 285 to 150°C, the most suitable $\alpha$ values are between 1 and 5°C min$^{-1}$.

The second experimental problem concerns the diameters of the measuring plates in order to have the best sensitivity over the six orders of magnitude of variation of the rheological parameters. According to the fourth-power dependence of torque on diameter $D$, it appears necessary to use at least two sets of plates with: $D=25$ mm initially for the molten state, and $D=8$ mm for $\eta^*>10^4$ Pa s. Thus it is necessary to perform two sets of experiments for each cooling rate, as carefully as possible in order to provide a good continuity at the connections.

A nitrogen thermoregulated draught is used to control the temperature and also to prevent—or minimize—polymer degradation.

Samples are pellets of 1 mm, made from sheets pressed at 240°C. The sample is molten at 285°C for 6 min to remove the thermal history as previously determined.

Concerning the strain $\gamma$, the values are chosen in order to perform experiments in the linear viscoelastic domain. For this purpose, a preliminary study is made at 270°C, at $\omega=1$ and 100 rad s$^{-1}$, in order to determine, for each polymer, the limiting $\gamma$ value over which the rheological parameters decrease. According to these results, drying conditions and rheological kinetics are carried out with shearing frequencies $\omega=5$ rad s$^{-1}$ for both samples and strains $\gamma=20\%$ and 10% for sample A and sample B respectively. Furthermore, the influence of $\omega$ and $\gamma$ on the starting temperatures of the kinetics is studied for the cooling rate $\alpha=3$°C min$^{-1}$ by means of an experimental design. Thus a central composite design is performed, according to the nine combinations of experimental factors. The response surface is estimated by fitting a full second-order polynomial from a home-made least-squares regression computer program.

## RESULTS AND DISCUSSION

### *Drying conditions*

The well known high moisture sensitivity of the molecular parameters of PET necessitates this preliminary step in order to confirm the optimal drying conditions. *Figure 1* shows the evolution of $\eta^*$ *versus* the drying time at 150°C under vacuum of the original polymer left in open air and containing 0.4% weight moisture. After 6 h, the values increase from 20 to 200 Pa s for PET A and from 10 to 95 Pa s for PET B; thereafter they remain constant. If such dried samples are held at 105°C in an air oven, these values stay constant for many months, at least two years, as previously observed for the crystallization endotherms[14].

According to Bueche[15] the dependence of viscosity on molecular weight is:

$$\eta_0=KM_w^a$$

with a theoretical value $a=3.4$ for monomolecular polymers[16]. As PET is Newtonian in our conditions, $\eta_0$ is close to $\eta^*$ and thus:

$$\eta^*=K'M_w^{a'} \quad (3)$$

PET A and B are linear polycondensates and present similar low polymolecularity ratio $I_p\approx2$. Thus from

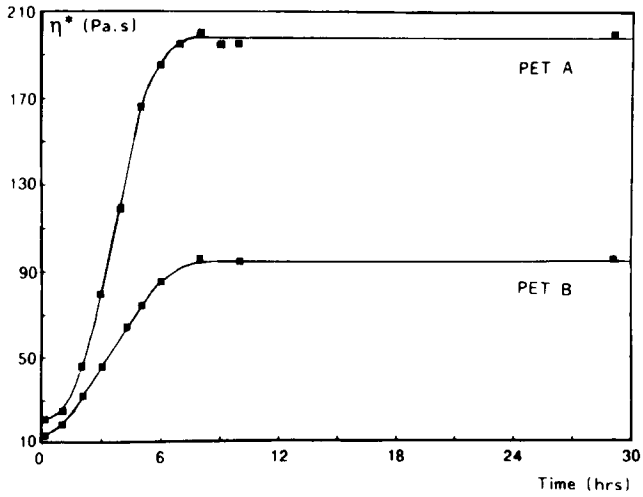


**Figure 1** Plot of the dynamic viscosity *versus* drying time at 150°C under vacuum for PET A and PET B

equation (3):

$$\frac{\eta_A^*}{\eta_B^*} = \left(\frac{M_{wA}}{M_{wB}}\right)^{a'}$$

From g.p.c. values $a' = 3.34$, which agrees well with the theory.

Equation (3) allows us also to compare hydrolysed and dried samples from the ratio $I$ of their respective molecular weights. For sample A and sample B the values obtained are respectively:

$$I_A = 1.99 \quad \text{and} \quad I_B = 1.96$$

In order to confirm the collapse of the molecular weights, the viscosity was measured, according to equation (2); both polymers show quite comparable values:

$$I_A = 1.88 \quad \text{and} \quad I_B = 1.87$$

We have therefore confirmed the importance of careful drying of this kind of polycondensate before any high-temperature treatment.

*Thermal stability*

Besides the effect of moisture, high temperatures and the surrounding atmosphere can also modify the properties of PET.

For temperatures higher than 250°C, with an air draught in the rheometer, $\eta^*$ and $G'$ decrease for both polymers previously dried. This may be due mainly to oxidative degradation. On the contrary, if nitrogen is used, $\eta^*$ and $G'$ increase in time for both PET samples; the highest increase occurs at 290°C and at about 100% in 45 min for $\eta^*$. It is negligible under 260°C and, for temperatures higher than 290°C, not used in this work, it decreases again. This evolution can be interpreted in terms of competition between post-polycondensation of the polycondensate and thermal degradation including also crosslinking of chains.

For our purpose, this phenomenon is sufficiently weak for the time during which the polymer is kept at over 260°C. The worst case is for the cooling rate value $\alpha = 1°C\,min^{-1}$. For this case, a higher initial cooling rate limits the evolution of $\eta^*$ to the acceptable value of 20%. It is worth noting that the thermal stabilizer used for PET B does not seem to have a significant effect in this temperature range.

*Rheological kinetics*

The complete rheological kinetics of both sample types at scanning rates ranging from 1 to $5°C\,min^{-1}$ give similar results. *Figure 2* reports the plots obtained for PET B at $3°C\,min^{-1}$. It is worth noting the good connection between the two experiments, as $3°C\,min^{-1}$ corresponds to the worst result. On each plot, three regions may be distinguished according to the decreasing temperature values.

(i) The first high-temperature part, over 225–230°C, corresponds to the molten state for which the viscosity—and also $\eta^*$—dependence is of Arrhenius type, i.e. linear *versus* $1/T$.

(ii) The second part, of sigmoidal appearance for each plot, begins at the starting temperature point ($T'_\alpha$ for $\eta^*$ and $T''_\alpha$ for $G'$) depending on the polymer type and on the cooling rate. The parameters $\eta^*$, $G'$ and $G''$ rapidly rise although tan $\delta$ decreases. *Figure 3* compares, for PET B, the plots of $\eta^*$ for three cooling rates: these plots seem to be simply shifted along the temperature axis. For PET A and PET B, $\eta^*$ plots are presented on *Figure 4*.

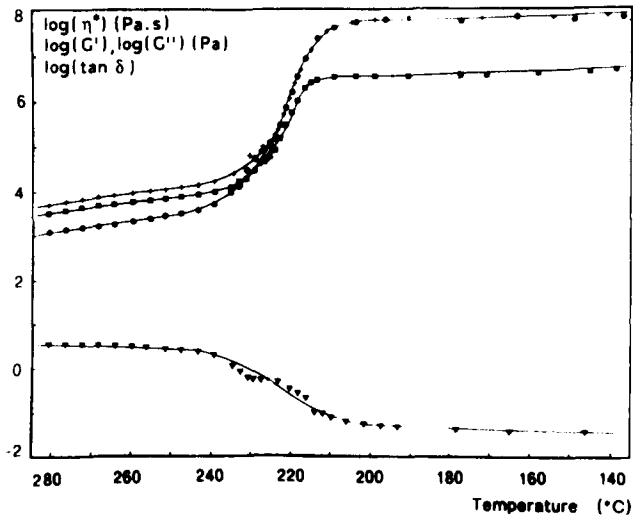


**Figure 2** Evolution of the rheological parameters *versus* temperature for PET B in anisothermal cooling conditions at $3°C\,min^{-1}$. The left part corresponds to a plate diameter of 25 mm, the right part to a diameter of 8 mm

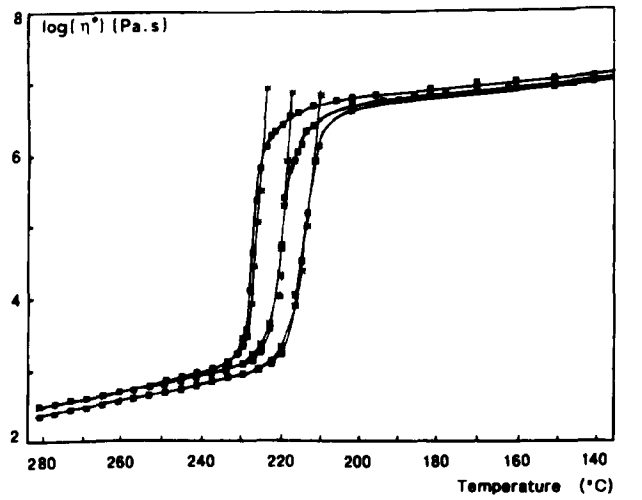


**Figure 3** Comparative plots of the dynamic viscosity for three cooling rates, respectively, 1, 3 and $5°C\,min^{-1}$ from left to right: (■) experimental values; (*) calculated values according to equation (7)

(iii) The last part, situated at temperatures lower than 190°C, characterizes the rubbery semicrystalline state of the polymers. For both types of samples and for every cooling rate, $G'$ and $\eta^*$ present the same values according to temperature. This was interpreted by Flocke[17] and Passaglia and Martin[18] in terms of final crystallinities. In our case, crystallinity measurements made by d.s.c. at a heating rate of $10°C\,min^{-1}$ give similar values for all solids in their final states. The crystallinity ratios are indeed in the range from 38 to 42% and thus confirm this interpretation.

The decrease of tan $\delta$ compared to the increase of the elastic modulus and the viscosity can be easily interpreted as a more and more elastic behaviour of the materials during crystallization[9].

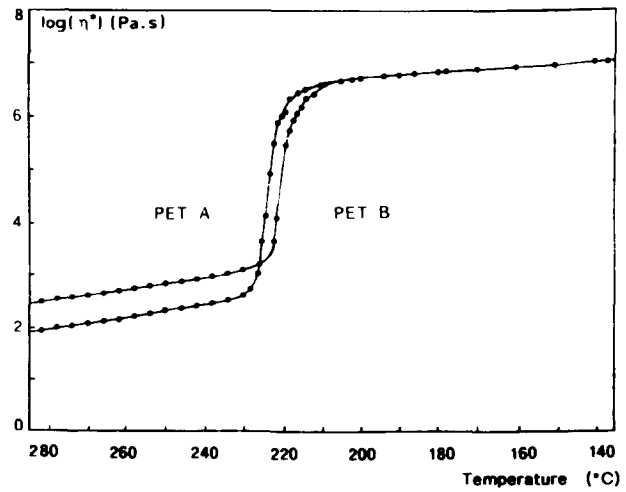


**Figure 4** Plot of viscosity *versus* temperature for PET A and PET B at 3°C min$^{-1}$

**Table 1** Starting temperature values for different cooling rates

| | PET A | | | PET B | | |
|---|---|---|---|---|---|---|
| $\alpha$(°C min$^{-1}$) | $T_\alpha$(d.s.c.) | $T'_\alpha(\eta^*)$ | $T''_\alpha(G')$ | $T_\alpha$(d.s.c.) | $T'_\alpha(\eta^*)$ | $T''_\alpha(G')$ |
| 1 | 238.4 | 238.2 | 240.9 | 231.6 | 232.2 | 234.5 |
| 2 | 235.2 | 235.6 | 239.2 | 228.8 | 229.5 | 232.2 |
| 3 | 234.6 | 233.9 | 237.5 | 225.5 | 227.4 | 230.1 |
| 4 | 233.6 | 232.5 | 236.5 | 223.5 | 224.9 | 228.7 |
| 5 | 231.2 | 231.1 | 235.4 | 222.1 | 223.1 | 227.6 |

**Table 2** Calculated coefficients of equation (7)

| $\alpha$(°C min$^{-1}$) | 1 | 3 | 5 |
|---|---|---|---|
| a | 9584 | 7515 | 7030 |
| b | −11.86 | −7.9 | −7.28 |
| c | 0.535 | 0.392 | 0.391 |
| d | −0.814 | −2.341 | −1.63 |

The last conclusion concerns the relative positions of the plots of PET A and PET B on *Figure 4*. As PET A presents a lower viscosity in the molten state, in accordance with its lower molecular weight, crystallization occurs at higher temperature than for PET B.

Despite the experimental difficulties, these data are quite accurate. This allows us to consider now the modelling of the phenomenon according to the experimental parameters $\alpha$, $\omega$ and $\gamma$. As no theoretical relations are available, these models will be completely empirical.

## MODELLING

*Temperature influence*

The first problem concerns the determinations of the starting point of each sigmoidal plot, $T'_\alpha$ and $T''_\alpha$ for $\eta^*$ and $G'$ respectively. Visual evaluations give values with a precision of approximately 0.4°C. For $\eta^*$, the first high-temperature part of the plot can be reported by the Arrhenius relation with $\eta^*$ close to $\eta_0$:

$$\ln \eta^* \approx \ln \eta_0 = a + b/T \tag{4}$$

where $T$ is the absolute temperature. A linear regression gives the values $a$ and $b$ with a correlation coefficient higher than 0.9999 for each plot. In the range $T < T'_\alpha$, a complementary function $f(T)$ can be added:

$$\ln \eta^* = a + b/T + f(T) \tag{5}$$

This relation is equivalent to:

$$\ln(\eta^*/\eta_0) = f(T)$$

where $\eta_0$ is the Arrhenius viscosity, assumed to be effective in the whole temperature range.

Inspired by the results of the crystallization kinetics, the following power law seems adequate for $f(T)$, for values close to $T'_\alpha$:

$$\ln(\eta^*/\eta_0) = A(T'_\alpha - T)^p \tag{6}$$

For $T < T'_\alpha$, it can be replaced by its polynomial expansion, more suited to determine the onset $T'_\alpha$. For all data, a polynomial of degree 2 is sufficient and the coefficients determined by least-squares regressions seem to correspond to a $p$ value close to 2. Calculated and observed $T'_\alpha$ values are summarized on *Table 1* and can be compared with the $T_\alpha$ from d.s.c.

Concerning the modelling of the phenomenon, we can assert, from practical considerations, that the most interesting part is the beginning, for $\eta^* < 10^5$ Pa s. The following equation can then be used:

$$\ln \eta^* = a/T + b + \exp[c(T'_\alpha - T) + d] \tag{7}$$

where $c$ and $d$ are coefficients. In this equation, the exponential function is continuous but presents negligible values for $T > T'_\alpha$ in the liquid state. Some calculated coefficients are summarized in *Table 2*. Plots of *Figure 3* present a comparison of experimental and calculated values, which are shown to correspond. For descriptions of the complete phenomenon, a more extended function can be conceived, for instance a derived form of the Avrami relation; yet one additional coefficient at least is necessary and no significant advantage is obtained. Moreover, this method gives less accurate results.

Concerning $G'$, relations analogous to equations (6) and (7) can be used and *Table 1* gives observed and calculated values for the starting point $T''_\alpha$ of $G'$. It is clearly seen that $T''_\alpha$ stays at least 2-7°C higher than the corresponding $T'_\alpha$ for $\eta^*$. A visual observation of the tan $\delta$ plot of *Figure 2* fully confirms this point: $G'$ is more sensitive to the early crystallization of the polymer, that is to say to the first appearance of the nuclei; the discrepancies between $T''_\alpha$ and $T'_\alpha$ seem to be higher at higher cooling rates. This confirms and completes the results from the literature[8,10]. Moreover, the elastic modulus is a parameter highly sensitive to early nucleation, which has a much weaker effect on other measurements such as endothermal heat.

The last point concerns the extension to $T'_\alpha$ and $T''_\alpha$ of the linear relation *versus* $\sqrt{\alpha}$, already established empirically for $T_\alpha$ from d.s.c. measurements. A complete plot is presented on *Figure 5* for PET A and B. In both cases, the linearity is confirmed and moreover the onsets are quite the same and the lines just differ from their slopes. These extrapolated neighbouring values $T_{0A} = 244.7 \pm 1.8$°C and $T_{0B} = 239.6 \pm 0.8$°C could be interpreted in terms of a boundary separating two crystallization mechanisms for

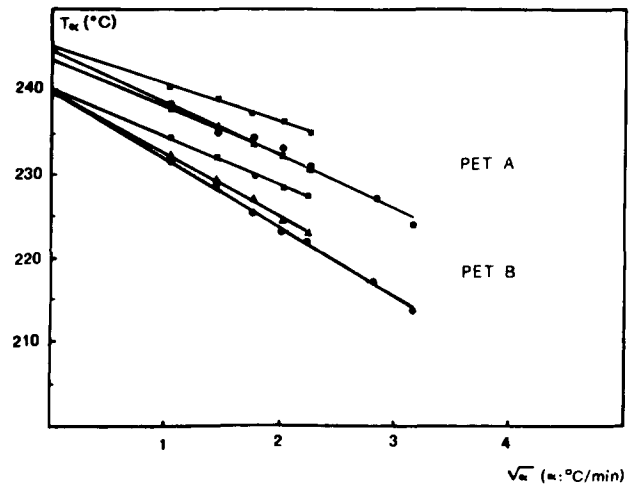


**Figure 5** Plot of starting temperature values *versus* $\sqrt{\alpha}$ for PET A and PET B: (■) for $G'$, (▲) for $\eta^*$, and (●) for d.s.c. measurements

which the delays, due to the nucleation steps, differ substantially. Thus at higher temperatures $T > T_0$ but $T < T_M$ (the limiting melting point, respectively 271°C and 274°C for A and B), the induction time is much larger than in the range $T < T_0$ and no crystallization can occur in a reasonable time. This was confirmed by hot-stage microscopy, for which the first observation of spherulites of PET B is 45 min at 245°C, 10 min at 240°C and 5 min at 235°C, from d.s.c. at 235°C this delay is 2 min. The literature also confirms this as a sizeable change of the Avrami exponents and the kinetic constants have indeed been observed for the crystallization of PET at temperatures higher than 240°C[19]. Our results seem to confirm the assumption that, under any anisothermal crystallization condition, a reference temperature is necessary in any relation describing it. This result is not in agreement with the theory for which the nucleation of the crystallization process occurs as soon as the temperature is lower than $T_M$.

*Shear influence*

As the starting value $T'_\alpha$ for $\eta^*$ seems to be slightly higher than the corresponding $T_\alpha$ observed for quiescent crystallization, the influence of the shearing strain $\gamma$ and the shearing frequency $\omega$ must then be studied in more detail. These parameters probably being correlated, a two-factor central composite design of second order seems to be well suited for relating their influences to $T'_\alpha$ and $T''_\alpha$ values according to:

$$T_\alpha - b_0 + b_1\omega + b_2\gamma + b_{11}\omega^2 + b_{22}\gamma^2 + b_{12}\omega\gamma \qquad (8)$$

where $b_i$ are characteristic coefficients. In this case, the set of measurements is often represented on a circle of radius $\sqrt{2}$, each axis being related to a factor that has five possible values. For each variable, the range must be as large as possible in order to have an extrapolation to the inaccessible value (0,0) as close as possible to the circle for the highest precision.

In order to test also the accuracy of the measurements, the centre of the circle corresponds to eight averaged experiments. As it is very tedious, only one set of measurements is carried out for PET B at $\alpha = 3°C\,min^{-1}$. *Table 3* gives the data of the experiments. The average value of the centre of the circle presents a standard deviation of 2°C. The full range for $T'_\alpha$ and $T''_\alpha$ is about 7°C, the highest values corresponding to higher nucleation rates[20]. Using a least-squares regression program, the $b_i$ coefficients are calculated and reported in *Table 4* (in uncoded, real units). The correlation coefficients are 0.995 and 0.992, and the standard deviation 0.37°C and 0.52°C, respectively, for $T'_\alpha$ and $T''_\alpha$. The response surfaces are of saddle type as shown by reducing the quadratic equations. It is worth noting that the coefficients $b_{22}$ show a strong correlation between $\omega$ and $\gamma$ for $\eta^*$ as for $G'$.

On *Table 3*, experimental and calculated values can be compared: the highest discrepancy is 0.6°C for $T'_\alpha$ and 0.9°C for $T''_\alpha$. Furthermore, the extrapolation at (0,0) gives the value $T'_\alpha = 225.6°C$, in good agreement with the d.s.c. measurements ($T_\alpha = 225.5°C$). It is also acceptable to compare calculated values $T'_\alpha = 226.3°C$, $T''_\alpha = 229.2°C$ and observed values $T'_\alpha = 227.4°C$, $T''_\alpha = 230.1°C$, from *Table 1* for the kinetics at $\omega = 5\ rad\ s^{-1}$ and $\gamma = 10\%$. This confirms the results of Lagasse and Maxwell[5] for polyethylene where no significant increase of nucleation rate occurs at low shearing.

**Table 3** Experimental design values

| Experiment | 1 | 2 | 3 | 4 | 5 | 6 | 7 | 8 | 9→16 |
|---|---|---|---|---|---|---|---|---|---|
| $\omega$ (rad s$^{-1}$) | 64.75 | 15.25 | 15.25 | 64.75 | 75 | 40 | 5 | 40 | 40 |
| $\gamma$ (%) | 78.3 | 78.3 | 21.71 | 21.71 | 50 | 90 | 50 | 10 | 50 |
| $T'_\alpha$ (measured) | 233.1 | 230.6 | 226.5 | 228.6 | 231.8 | 232.8 | 229.0 | 226.6 | 229.8 |
| $T'_\alpha$ (calculated) | 233.2 | 231.1 | 227.1 | 228.8 | 231.5 | 232.9 | 228.8 | 227.0 | 229.8 |
| $T''_\alpha$ (measured) | 236.8 | 234.7 | 229.7 | 230.9 | 234.3 | 235.4 | 230.5 | 229.6 | 231.8 |
| $T''_\alpha$ (calculated) | 236.4 | 233.8 | 229.5 | 231.2 | 234.2 | 236.2 | 231.2 | 229.4 | 231.8 |

**Table 4** Calculated coefficients of equation (8)

| Parameter | $b_0$ | $b_1$ | $b_2$ | $b_{11}$ | $b_{12}$ | $b_{22}$ |
|---|---|---|---|---|---|---|
| $T'_\alpha$ | 225.6 | $7.7 \times 10^{-3}$ | $5.8 \times 10^{-2}$ | $2.78 \times 10^{-4}$ | $8.52 \times 10^{-5}$ | $1.68 \times 10^{-4}$ |
| $T''_\alpha$ | 229.17 | $-3.02 \times 10^{-2}$ | $9.8 \times 10^{-3}$ | $7.25 \times 10^{-4}$ | $6.17 \times 10^{-4}$ | $3.21 \times 10^{-4}$ |

## CONCLUSION

The rheological kinetics has been studied for two classical PET materials. Despite all the difficulties, experimental results are satisfactory enough to model correctly the phenomena *versus* the three parameters: temperature (or cooling rate), shear and frequency. The last two parameters are strongly correlated but give a sensible variation in the kinetics only for substantially high values. Another interesting result is the evolution of the elastic modulus, which shows variations long before viscosity measurements because of its higher sensitivity to the increasing number of entanglements from the nuclei of crystallization.

Finally, rheological kinetics and crystallization kinetics can be correlated, although it is empirical, and attempts will be made to complete this point so as to make the model more theoretical.

## ACKNOWLEDGEMENTS

We wish to thank PSA for their financial support of this work. We are also grateful to Dr Gand for helpful suggestions concerning the experimental design.

## REFERENCES

1 Douillard, A., Dumazet, P., Chabert, B. and Guillet, J. *Polymer* 1993, **34**, 1702
2 Cogswell, F. N. *Int. Polym. Process.* 1987, **1**(4), 157
3 Greco, R. and Coppola, F. *Plast. Rubber Process. Applic.* 1986, **6**, 35
4 Harran, D. and Laudouard, A. *Rheol. Acta* 1985, **24**, 596
5 Lagasse, R. R. and Maxwell, B. *Polym. Eng. Sci.* 1976, **16**(3), 189
6 Fritzsche, A. K. and Price, F. P. *Polym. Eng. Sci.* 1974, **14**, 401
7 Price, F. P. 'Polymer Crystallization During Flow', General Electric Technical Information Series, Schenectady, NY, 1967
8 Haas, T. W. and Maxwell, B. *Polym. Eng. Sci.* 1969, **9**, 225
9 Kushner, B. and Chang, E.-P. *Polym. Eng. Sci.* 1979, **19**(16), 1170
10 Fritzsche, A. K., Price, F. P. and Ulrich, R. D. *Am. Chem. Soc. Polym. Prepr.* 1975, **16**, 395
11 Avrami, M. *J. Chem. Phys.* 1939, **7**, 1103; 1940, **8**, 212
12 Evans, M. *Trans. Faraday Soc.* 1945, **41**, 365
13 Rhodes, M. B. and Stein, R. S. *J. Appl. Polym. Sci.* 1960, **31**, 1873
14 Dumazet, P., Chabert, B., Douillard, A., Guillet, J., Gerard, A. and Andre, G. III European Polymer Federation Congress, Sorrento, Italy, 1990, p. 130
15 Bueche, F. *J. Chem. Phys.* 1952, **20**, 1959
16 Montfort, J. P. *Polymer* 1976, **17**, 1054
17 Flocke, H. A. *Kolloid Z.* 1962, **180**, 118
18 Passaglia, E. and Martin, G. M. *J. Res. NBS* 1964, **68**, 519
19 Wunderlich, B. *Macromol. Phys.* 1976, **2**, 241
20 Jabarin, S. A. and Logfren, E. A. *Polym. Eng. Sci.* 1984, **24**(13), 1056